4 Static Body Stresses

4.1 Introduction

Once the external *loads* applied to a member have been determined (see Chapter 2), the next item of interest is often the resulting *stresses*. This chapter is concerned with *body* stresses, existing within the member as a whole, as distinguished from *surface* or *contact* stresses in localized regions where external loads are applied. This chapter is also concerned with stresses resulting from essentially *static* loading, as opposed to stresses caused by impact or fatigue loading. (Impact, fatigue, and surface stresses are considered in Chapters 7, 8, and 9, respectively.)

As noted in Section 3.2, this book follows the convention of reserving the capital letter S for *material strength* (i.e., S_u for ultimate strength, S_y for yield strength, etc.) and using Greek letters σ and τ for normal and shear stress, respectively.

4.2 Axial Loading

Figure 4.1 illustrates a case of simple *tension*. If external loads P are reversed in direction (i.e., have negative values), the bar is loaded in simple *compression*. In either case, the loading is *axial*. Small block E represents an arbitrarily located infinitesimally small element of material that is shown by itself in Figures 4.1*b* and *c*. Just as equilibrium of the bar as a whole requires the two external forces P to be equal, equilibrium of the element requires the tensile stresses acting on the opposite pair of elemental faces to be equal. Such elements are commonly shown as in Figure 4.1*c*, where it is important to remember that the stresses are acting on faces *perpendicular to the paper*. This is made clear by the isometric view in Figure 4.1*b*.

Figure 4.1*d* illustrates equilibrium of the left portion of the link under the action of the external force at the left and the tensile stresses acting on the cutting plane. From this equilibrium we have perhaps the simplest formula in all of engineering:

$$\sigma = P/A \tag{4.1}$$

It is important to remember that although this formula is always correct as an expression for the *average* stress in any cross section, disastrous errors can be made by naively assuming that it also gives the correct value of *maximum* stress in the section. Unless several important requirements are fulfilled, the maximum stress will be

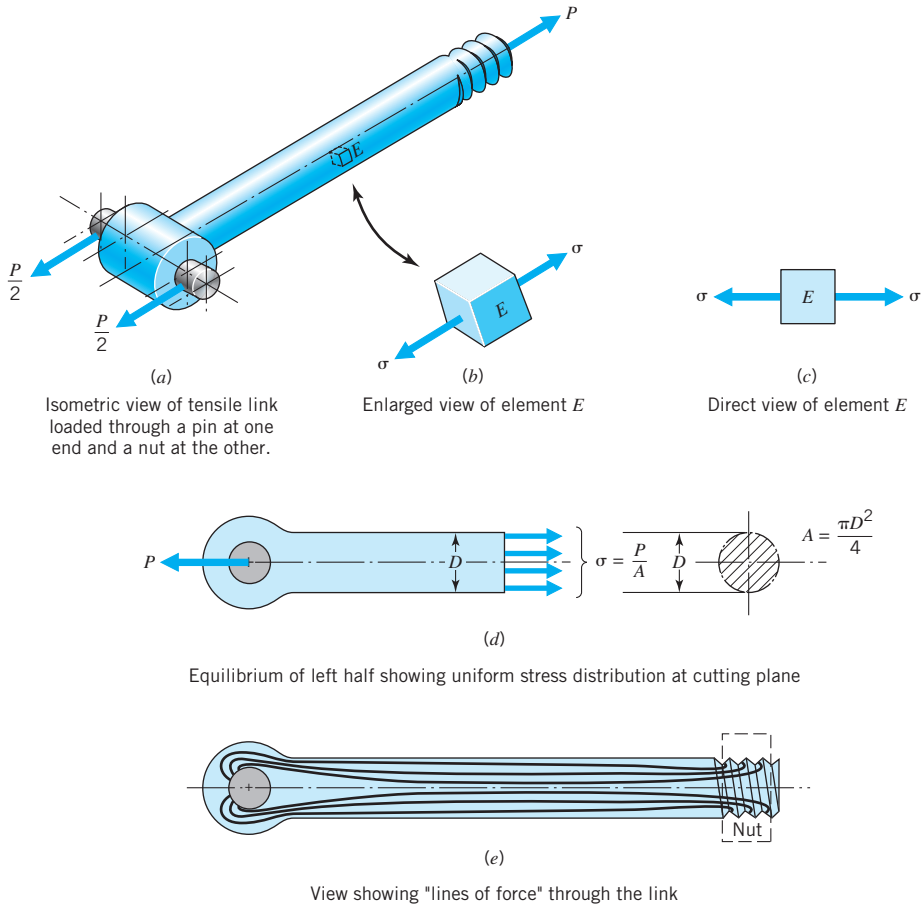

FIGURE 4.1
Axial loading.

greater than *P*/*A*, perhaps by several hundred percent. The maximum stress is equal to *P*/*A* only if the load is *uniformly distributed* over the cross section. This requires the following.

1. The section being considered is well removed from the loaded ends. Figure 4.1*e* shows "lines of force flow" to illustrate the general nature of the stress distribution in cross sections at various distances from the ends. A substantially uniform distribution is reached at points about three diameters from the end fittings in most cases.
2. The load is applied *exactly* along the centroidal axis of the bar. If, for example, the loads are applied a little closer to the top, the stresses will be highest at the top of the bar and lowest at the bottom. (Looking at it another way, if the load is eccentric by amount *e*, a bending moment of intensity *Pe* is superimposed on the axial load.)
3. The bar is a perfect straight cylinder, with no holes, notches, threads, internal imperfections, or even surface scratches. Any of these give rise to *stress concentration*, which will be dealt with in Section 4.12.

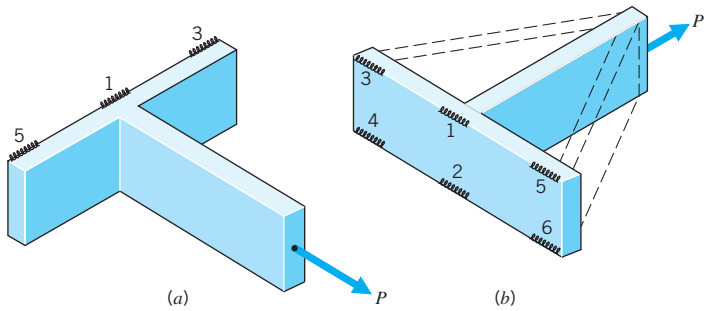

FIGURE 4.2
Tensile-loaded T bracket attached by six welds.

4. The bar is totally free of stress when the external loads are removed. This is frequently not the case. The manufacture of the part and its subsequent mechanical and thermal loading history may have created *residual stresses*, as described in Sections 4.14, 4.15, and 4.16.
5. The bar comes to stable equilibrium when loaded. This requirement is violated if the bar is relatively long and loaded in compression. Then it becomes elastically unstable, and *buckling* occurs. (See Sections 5.10 through 5.15.)
6. The bar is homogeneous. A common example of *non* homogeneity is a composite material, such as glass or carbon fibers in a plastic matrix. Here the matrix and the fibers carry the load *redundantly* (see Section 2.5), and the stiffer material (i.e., having the higher modulus of elasticity) is the more highly stressed.

Figure 4.2 shows an example in which unexpected failure can easily result from the naive assumption that the calculation of axial stress involves no more than "*P*/*A*." Suppose that the load *P* is 600 N and that six identical welds are used to attach the bracket to a fixed flat surface. The *average* load per weld would be, of course, 100 N. However, the six welds represent redundant force paths of very different stiffnesses. The paths to welds 1 and 2 are *much* stiffer than the others; hence, these two welds may carry nearly all the load. A much more uniform distribution of load among the six welds could be obtained by adding the two side plates shown dotted in Figure 4.2*b*, for these would stiffen the force paths to welds 3 to 6.

At this point one might despair of *ever* using *P*/*A* as an acceptable value of maximum stress for relating to the strength properties of the material. Fortunately, such is not the case. The student should acquire increasing insight for making "engineering judgments" relative to these factors as his or her study progresses and experience grows.

4.3 Direct Shear Loading

Direct shear loading involves the application of equal and opposite forces so nearly colinear that the material between them experiences shear stress, with negligible bending. Figure 4.3 shows a bolt serving to restrain relative sliding of two plates subjected to opposing forces *P*. With plate interface friction neglected, the bolt cross section of area *A* (marked ①) experiences direct shear stress of *average* value

$$\tau = P/A \tag{4.2}$$

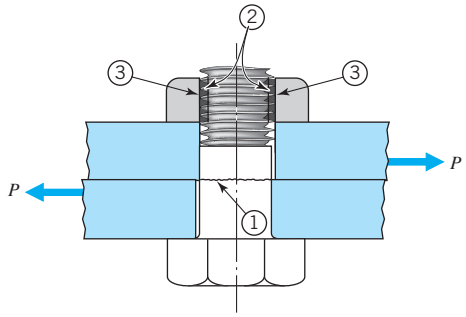

FIGURE 4.3
Bolted joint, showing three areas of direct shear.

If the nut in Figure 4.3 is tightened to produce an initial bolt tension of P, the direct shear stresses at the root of the bolt threads (area ②), and at the root of the nut threads (area ③), have *average* values in accordance with Eq. 4.2. The thread root areas involved are cylinders of a height equal to the nut thickness.[1] If the shear stress is excessive, shearing or "stripping" of the threads occurs in the bolt or nut, whichever is weaker.

Similar examples of direct shear occur in rivets, pins, keys, splines, and so on. Moreover, direct shear loading is commonly used for cutting, as in ordinary household *shears* or scissors, paper cutters, and industrial metal shears.

Figure 4.4 shows a hinge pin loaded in *double* shear, where the load P is carried in shear through two areas in parallel; hence, the area A used in Eq. 4.2 is *twice* the cross-sectional area of the pin. Examples of pins loaded in double shear are common: cotter pins used to prevent threaded nuts from rotating (as with automobile wheel bearing retaining nuts), shear pins used to drive boat propellers (the pin fails in double shear when the propeller strikes a major obstruction, thus protecting more expensive and difficult-to-replace members), transverse pins used to hold telescoping tubular members in a fixed position, and many others.

Direct shear loading does not produce *pure* shear (as does torsional loading), and the actual stress distribution is complex. It involves fits between the mating members and relative stiffnesses. The maximum shear stress will always be somewhat in excess of the P/A value given by Eq. 4.2. In the design of machine and structural members, however, Eq. 4.2 is commonly used in conjunction with appropriately conservative values of working shear stress. Furthermore, to produce total shear fracture of a ductile member, the load must simultaneously overcome the shear strength in every element of material in the shear plane. Thus, for total fracture, Eq. 4.2 would apply, with τ being set equal to the ultimate shear strength, S_{us}.

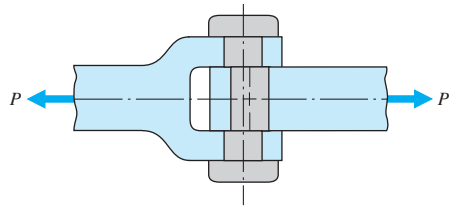

FIGURE 4.4
Direct shear loading (showing failure in double shear).

[1] Strictly true only for threads with a sharp "V" profile. Shear areas for standard threads are a little less. See Section 10.4.5.

4.4 Torsional Loading

Figure 4.5 illustrates torsional loading of a round bar. Note that the direction of the applied torque (T) determines that the left face of element E is subjected to a *downward* shear stress, and the right face to an *upward* stress. Together, these stresses exert a *counterclockwise* couple on the element that must be balanced by a corresponding *clockwise* couple, created by shear stresses acting on the top and bottom faces. The state of stress shown on element E is *pure shear*.

The sign convention for axial loading (positive for tension, negative for compression) distinguishes between two basically different types of loading: compression can cause buckling whereas tension cannot, a chain or cable can withstand tension but not compression, concrete is strong in compression but weak in tension, and so on. The sign convention for *shear* loading serves no similar function—positive and negative shear are basically the same—and the sign convention is purely arbitrary. Any shear sign convention is satisfactory so long as the *same* convention is used throughout any one problem. This book uses the convention of *positive-clockwise*; that is, the shear stresses on the top and bottom faces of element E (in Figure 4.5) tend to rotate the element *clockwise*, hence are regarded as *positive*. The vertical faces are subjected to *counterclockwise* shear, which is *negative*.

For a round bar in torsion, the stresses vary linearly from zero at the axis to a maximum at the outer surface. Strength of materials texts contain formal proofs that the shear stress intensity at any radius r is

$$\tau = Tr/J \tag{4.3}$$

Of particular interest, of course, is the stress at the surface, where r is equal to the outside radius of the bar and J is the polar moment of inertia of the cross section, which is equal to $\pi d^4/32$ for a solid round bar of diameter d (see Appendix B-1). Simple substitution of this expression in Eq. 4.3 gives the equation for surface torsional stress in a solid round bar of diameter d:

$$\tau_{\max} = 16T/\pi d^3 \tag{4.4}$$

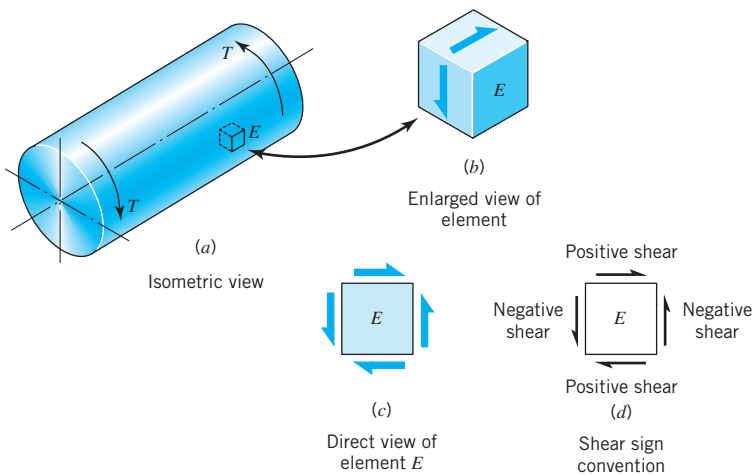

FIGURE 4.5
Torsional loading of a round bar.

The corresponding equation for torsional stress in a *hollow* round bar (i.e., round tubing or pipe) follows from substitution of the appropriate equation for polar moment of inertia (see Appendix B-1).

The important assumptions associated with Eq. 4.3 are

1. The bar must be straight and round (either solid or hollow), and the torque must be applied about the longitudinal axis.
2. The material must be homogeneous and perfectly elastic within the stress range involved.
3. The cross section considered must be sufficiently remote from points of load application and from stress raisers (i.e., holes, notches, keyways, surface gouges, etc.).

For bars of nonround cross section, the foregoing analysis gives *completely* erroneous results. This can be demonstrated for rectangular bars by marking an ordinary rubber eraser with small square elements 1, 2, and 3 as shown in Figure 4.6. When the eraser is twisted about its longitudinal axis, Eq. 4.3 implies that the highest shear stress would be at the corners (element 2) because these are farthest from the neutral axis. Similarly, the lowest surface stress should be at element 1 because it is closest to the axis. Observation of the twisted eraser shows exactly the opposite—element 2 (if it could be drawn small enough) does not distort at all, whereas element 1 experiences the *greatest* distortion of any element on the entire surface!

A review of a formal derivation of Eq. 4.3 reminds us of the basic assumption that *what are transverse planes before twisting remain planes after twisting*. If such a plane is represented by drawing line "*A*" on the eraser, obvious distortion occurs upon twisting; therefore, the assumption is not valid for a rectangular section.

The equilibrium requirement of corner element 2 makes it clear that this element *must* have zero shear stress: (1) the "free" top and front surfaces do not contact anything that could apply shear stresses; (2) this being so, equilibrium requirements prevent any of the other four surfaces from having shear. Hence, there is zero shear stress along all edges of the eraser.

Torsional stress equations for nonround sections are summarized in references such as [8]. For example, the maximum shear stress for a rectangular section, as shown in Figure 4.6, is

$$\tau_{\max} = T(3a + 1.8b)/a^2b^2 \qquad \textbf{(4.5)}$$

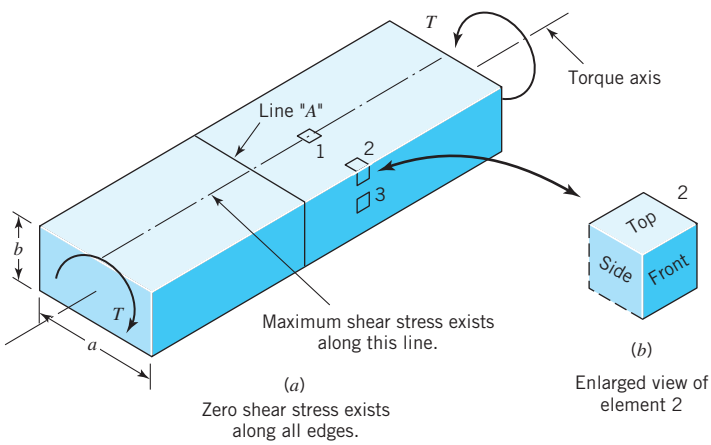

FIGURE 4.6
Rubber eraser marked to illustrate torsional deformation (hence stresses) in a rectangular bar.

4.5 Pure Bending Loading, Straight Beams

Figures 4.7 and 4.8 show beams loaded *only* in bending; hence the term, "pure bending." From studies of the strength of materials, the resulting stresses are given by the equation

$$\sigma = My/I \tag{4.6}$$

where I is the moment of inertia of the cross section with respect to the neutral axis, and y is the distance from the neutral axis. Bending stresses are *normal* stresses, the same as axial stresses. Sometimes the two are distinguished by using appropriate subscripts, as σ_b for bending stresses and σ_a for axial stresses. For the bending shown in Figures 4.7 and 4.8, tensile stresses exist above the neutral axis of the section (or above the neutral surface of the beam), and compressive stresses below. Maximum values are at the top and bottom surfaces.

Equation 4.6 applies to any cross section (such as the several that are illustrated), with these important limitations.

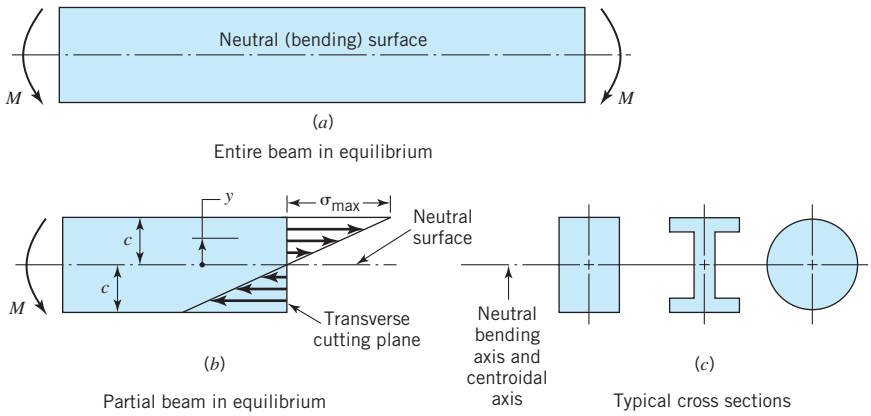

FIGURE 4.7
Pure bending of sections with two axes of symmetry.

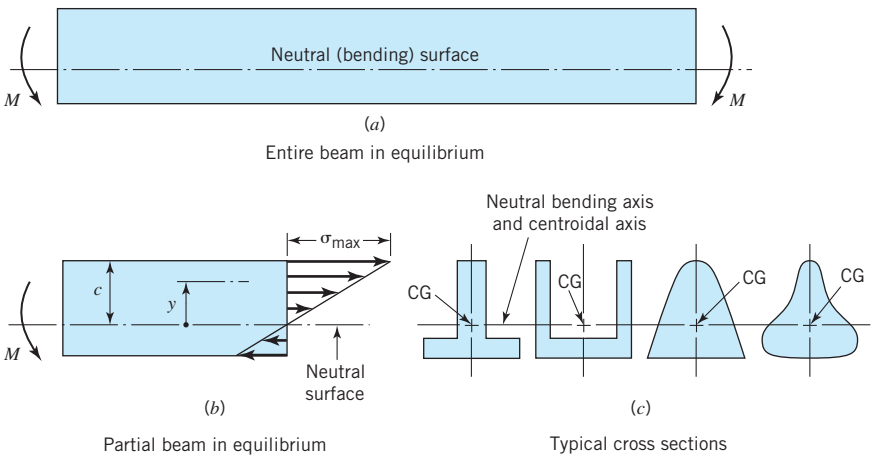

FIGURE 4.8
Pure bending of sections with one axis of symmetry.

1. The bar must be initially straight and loaded in a plane of symmetry.
2. The material must be homogeneous, and all stresses must be within the elastic range.
3. The section for which stresses are calculated must not be too close to significant stress raisers or to regions where external loads are applied.

Figure 4.7 shows a bending load applied to a beam of cross section having two axes of symmetry. Note that the cutting-plane stresses marked σ_{max} are obtained from Eq. 4.6 by substituting c for y, where c is the distance from the neutral axis to the extreme fiber. Often the *section modulus* Z (defined as the ratio I/c) is used, giving the equation for maximum bending stress as

$$\sigma_{max} = M/Z = Mc/I \tag{4.7}$$

For a solid round bar, $I = \pi d^4/64$, $c = d/2$, and $Z = \pi d^3/32$. Hence, for this case

$$\sigma_{max} = 32M/\pi d^3 \tag{4.8}$$

Properties of various cross sections are given in Appendix B-1.

Figure 4.8 shows bending of sections having a single axis of symmetry, and where the bending moment lies in the plane containing the axis of symmetry of each cross section. At this point the reader will find it profitable to spend a few moments verifying that the offset stress distribution pattern shown is necessary to establish equilibrium in Figure 4.8*b* (i.e., $\Sigma F = \Sigma \sigma\, dA = 0$, and $\Sigma M = M + \Sigma \sigma\, dA\, y = 0$).

4.6 Pure Bending Loading, Curved Beams

When initially curved beams are loaded in the plane of curvature, the bending stresses are only approximately in accordance with Eqs. 4.6 through 4.8. Since the shortest (hence stiffest) path along the length of a curved beam is at the inside surface, a consideration of the relative stiffnesses of redundant load paths suggests that the stresses at the inside surface are *greater* than indicated by the straight-beam equations. Figure 4.9 illustrates that this is indeed the case. This figure also shows that equilibrium requirements cause the neutral axis to shift inward (toward the center of curvature) an amount e, and the stress distribution to become hyperbolic. These deviations from straight-beam behavior are important in severely curved beams, such as those commonly encountered in C-clamps, punch press and drill press frames, hooks, brackets, and chain links.

To understand more clearly the behavior pattern shown in Figure 4.9*c*, let us develop the basic curved-beam stress equations. With reference to Figure 4.10, let *abcd* represent an element bounded by plane of symmetry *ab* (which does not change direction when moment M is applied) and plane *cd*. Moment M causes plane *cd* to rotate through angle $d\phi$ to new position $c'd'$. (Note the implied assumption that plane sections remain plane after loading.) Rotation of this plane is, of course, about the neutral bending axis, displaced an as-yet-unknown distance e from the centroidal axis.

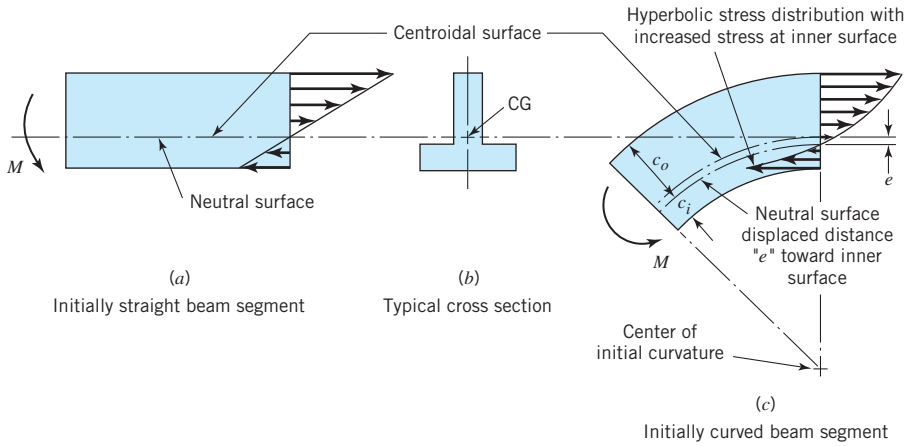

FIGURE 4.9
Effect of initial curvature, pure bending of sections with one axis of symmetry.

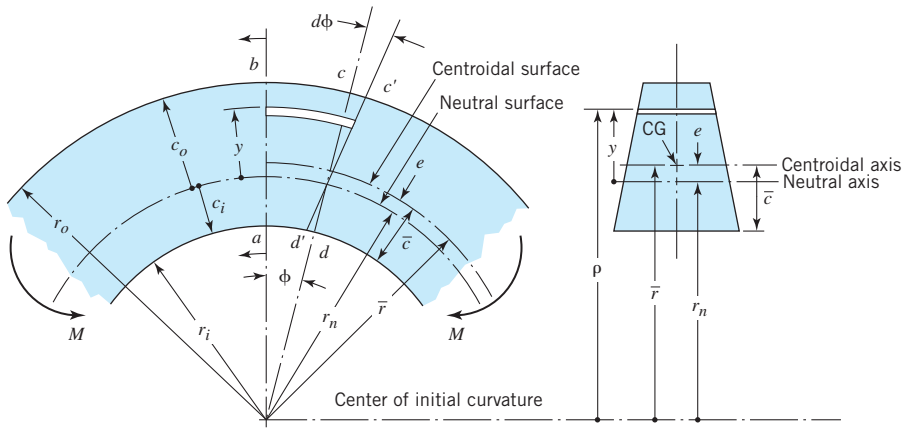

FIGURE 4.10
Curved beam in bending.

The strain on the fiber shown at distance y from the neutral axis is

$$\epsilon = \frac{y\,d\phi}{(r_n + y)\phi} \tag{a}$$

For an elastic material, the corresponding stress is

$$\sigma = \frac{Ey\,d\phi}{(r_n + y)\phi} \tag{b}$$

Note that this equation gives a hyperbolic distribution of stress, as illustrated in Figure 4.9*c*.

Equilibrium of the beam segment on either side of plane *cd* (Figure 4.10) requires

$$\Sigma F = 0: \quad \int \sigma \, dA = \frac{E \, d\phi}{\phi} \int \frac{y \, dA}{r_n + y} = 0$$

and, since $E \neq 0$,

$$\int \frac{y \, dA}{r_n + y} = 0 \tag{c}$$

$$\Sigma M = 0: \quad \int \sigma y \, dA = \frac{E \, d\phi}{\phi} \int \frac{y^2 \, dA}{r_n + y} = M \tag{d}$$

The quantity $y^2/(r_n + y)$ in Eq. d can be replaced by $y - r_n y/(r_n + y)$, giving

$$M = \frac{E \, d\phi}{\phi} \left(\int y \, dA - r_n \int \frac{y \, dA}{r_n + y} \right) \tag{e}$$

The second integral in Eq. e is equal to zero because of Eq. c. The first integral is equal to eA. (Note that this integral would be equal to zero if y were measured from the centroidal axis. Since y is measured from an axis displaced distance e from the centroid, the integral has a value of eA.)

Substituting the preceding expressions into Eq. e gives

$$M = \frac{E \, d\phi}{\phi} eA \quad \text{or} \quad E = \frac{M\phi}{d\phi \, eA} \tag{f}$$

Substituting Eq. f into Eq. b gives

$$\sigma = \frac{My}{eA(r_n + y)} \tag{g}$$

Substituting $y = -c_i$ and $y = c_o$ in order to find maximum stress values at the inner and outer surfaces, we have

$$\sigma_i = \frac{-Mc_i}{eA(r_n - c_i)} = \frac{-Mc_i}{eAr_i}$$

$$\sigma_o = \frac{Mc_o}{eA(r_n + c_o)} = \frac{Mc_o}{eAr_o}$$

The signs of these equations are consistent with the compressive and tensile stresses produced in the inner and outer surfaces of the beam in Figure 4.10, where

the direction of moment M was chosen in the interest of clarifying the analysis. More commonly, a positive bending moment is defined as one tending to *straighten* an initially curved beam. In terms of this convention,

$$\sigma_i = +\frac{Mc_i}{eAr_i} \quad \text{and} \quad \sigma_o = -\frac{Mc_o}{eAr_o} \tag{4.9}$$

Before we use Eq. 4.9, it is necessary to develop an equation for distance e. Beginning with the force equilibrium requirement, Eq. c, and substituting ρ for $r_n + y$, we have

$$\int \frac{y\,dA}{\rho} = 0$$

But $y = \rho - r_n$; hence,

$$\int \frac{(\rho - r_n)\,dA}{\rho} = 0$$

or

$$\int dA - \int \frac{r_n\,dA}{\rho} = 0$$

Now $\int dA = A$; hence,

$$A = r_n \int dA/\rho \quad \text{or} \quad r_n = \frac{A}{\int dA/\rho} \tag{h}$$

Distance e is equal to $\bar{r} - r_n$; hence,

$$e = \bar{r} - \frac{A}{\int dA/\rho} \tag{4.10}$$

Stress values given by Eq. 4.9 differ from the straight-beam "Mc/I" value by a curvature factor, K. Thus, using subscripts i and o to denote inside and outside fibers, respectively, we have

$$\sigma_i = K_i Mc/I = K_i M/Z \quad \text{and} \quad \sigma_0 = -K_o Mc/I = -K_o M/Z \tag{4.11}$$

where c is defined in Figure 4.8.

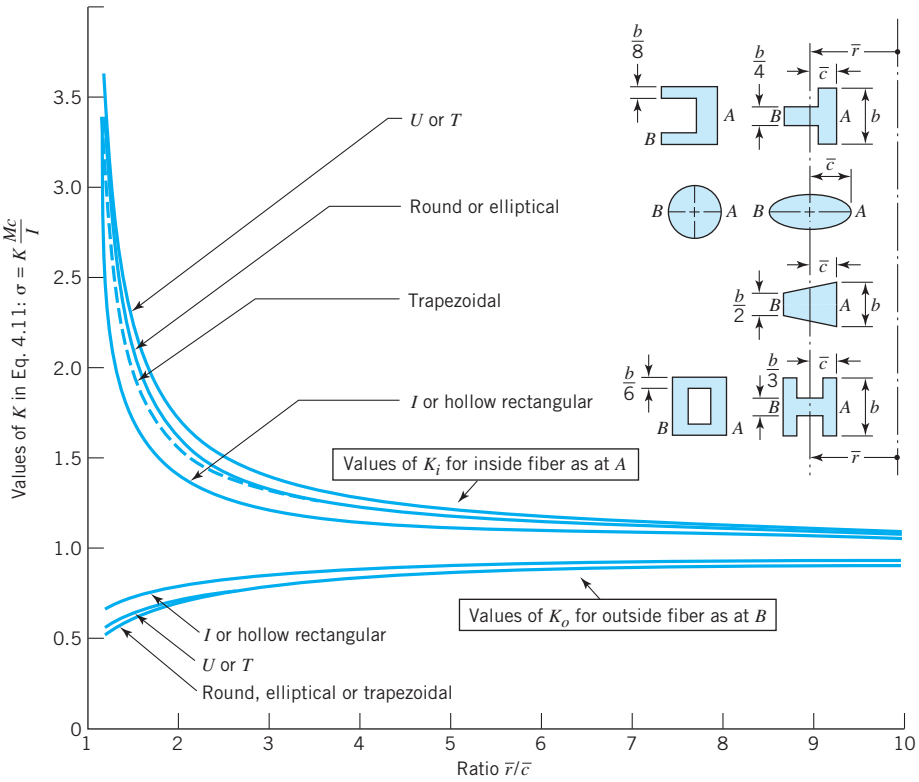

FIGURE 4.11
Effect of curvature on bending stresses, representative cross sections [8].

Values of K for beams of representative cross sections and various curvatures are plotted in Figure 4.11. This illustrates a common rule of thumb: "If $\bar{r}$ is at least ten times $\bar{c}$, inner fiber stresses are usually not more than 10 percent above the Mc/I value." Values of K_o, K_i, and e are tabulated for several cross sections in [8]. Of course, any section can be handled by using Eqs. 4.9 and 4.10. If necessary, the integral in Eq. 4.10 can be evaluated numerically or graphically. Use of these equations is illustrated by the following sample problem.

SAMPLE PROBLEM 4.1 Bending Stresses in Straight and Curved Beams

A rectangular beam has an initial curvature $\bar{r}$ equal to the section depth h, as shown in Figure 4.12. How do its extreme-fiber-bending stresses compare with those of an otherwise identical straight beam?

SOLUTION

Known: A straight beam and a curved beam of given cross section and initial curvature are loaded in bending.

Find: Compare the bending stresses between the straight beam and the curved beam.

Schematic and Given Data:

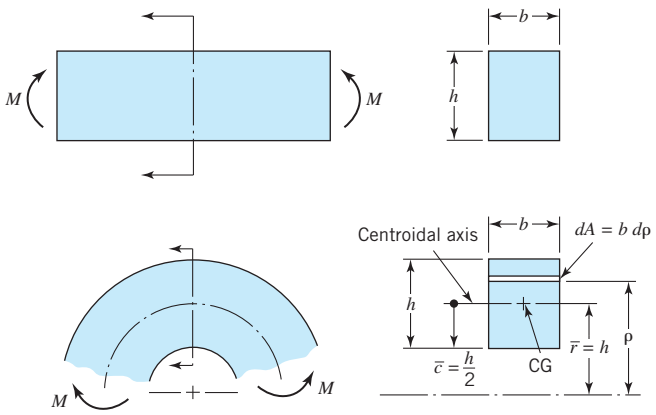

FIGURE 4.12
A curved rectangular bar with radius of curvature $\bar{r}$ equal to section depth h (giving $\bar{r}/\bar{c} = 2$) and a straight rectangular bar.

Assumptions:

1. The straight bar must initially be straight.
2. The beams are loaded in a plane of symmetry.
3. The material is homogeneous, and all stresses are within the elastic range.
4. The sections for which the stresses are calculated are not too close to significant stress raisers or to regions where external loads are applied.
5. Initial plane sections remain plane after loading.
6. The bending moment is positive; that is, it tends to straighten an initially curved beam.

Analysis:

1. For the direction of loading shown in Figure 4.12, the conventional straight-beam formula gives

$$\sigma_i = +\frac{Mc}{I} = \frac{6M}{bh^2}, \qquad \sigma_o = -\frac{6M}{bh^2}$$

2. From Eq. 4.10,

$$e = \bar{r} - \frac{A}{\int dA/\rho} = h - \frac{bh}{b\displaystyle\int_{r_i}^{r_o} d\rho/\rho} = h - \frac{h}{\ln(r_o/r_i)} = h\left(1 - \frac{1}{\ln 3}\right)$$

$$= 0.089761h$$

3. From Eq. 4.9,

$$\sigma_i = +\frac{M(0.5h - 0.089761h)}{(0.089761h)(bh)(0.5h)} = \frac{9.141M}{bh^2}$$

$$\sigma_o = -\frac{M(0.5h + 0.089761h)}{(0.089761h)(bh)(1.5h)} = -\frac{4.380M}{bh^2}$$

4. From Eq. 4.11 with $Z = bh^2/6$,

$$K_i = \frac{9.141}{6} = 1.52 \quad \text{and} \quad K_o = \frac{4.380}{6} = 0.73$$

Comment: These values are consistent with those shown for other sections in Figure 4.11 for $\bar{r}/\bar{c} = 2$.

Note that the stresses dealt with in the bending of curved beams are *circumferential*. Additionally, *radial* stresses are present that are, in some cases, significant. To visualize these, take a paper pad and bend it in an arc, as shown in Figure 4.13*a*. Apply compressive forces with the thumbs and forefingers so that the sheets will not slide. Next, carefully superimpose (with the thumbs and forefingers) a small bending moment, as in 4.13*b*. Note the separation of the sheets in the center of the "beam," indicating the presence of *radial tension* (radial compression for opposite bending). These radial stresses are small if the center portion of the beam is reasonably heavy. But for an I beam with a thin web, for example, the radial stresses can be large enough to cause damage—particularly if the beam is made of a brittle material or is subjected to fatigue loading. Further information on curved-beam radial stresses is contained in [8] and [9].

4.7 Transverse Shear Loading in Beams

Although the *average* transverse shear stress in beams such as the shaft in Chapter 2, Figure 2.11 is equal to *V*/*A* (i.e., 1580 lb divided by the cross-sectional area in the critical shaft section shown in Figure 2.12), the *maximum* shear stress is substantially higher. We will now review an analysis of the distribution of this transverse shear stress, with emphasis on an understanding of the basic concepts involved.

Figure 4.14 shows a beam of an arbitrary cross section that is symmetrical about the plane of loading. It is supported at the ends and carries a concentrated load at the center. We wish to investigate the distribution of transverse shear stress in a plane located distance *x* from the left support, and at a distance *y* above the neutral axis. A small square element at this location is shown in the upper right drawing. The right and left faces of the element are subjected to shear stresses (the magnitude of which is to be determined) with directions established by the fact that the only external force to the left of the element is directed upward, and the resultant of external forces

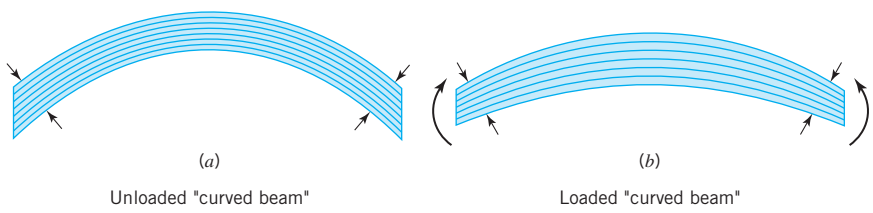

FIGURE 4.13
Paper pad illustrating radial tension in a curved beam loaded in bending.

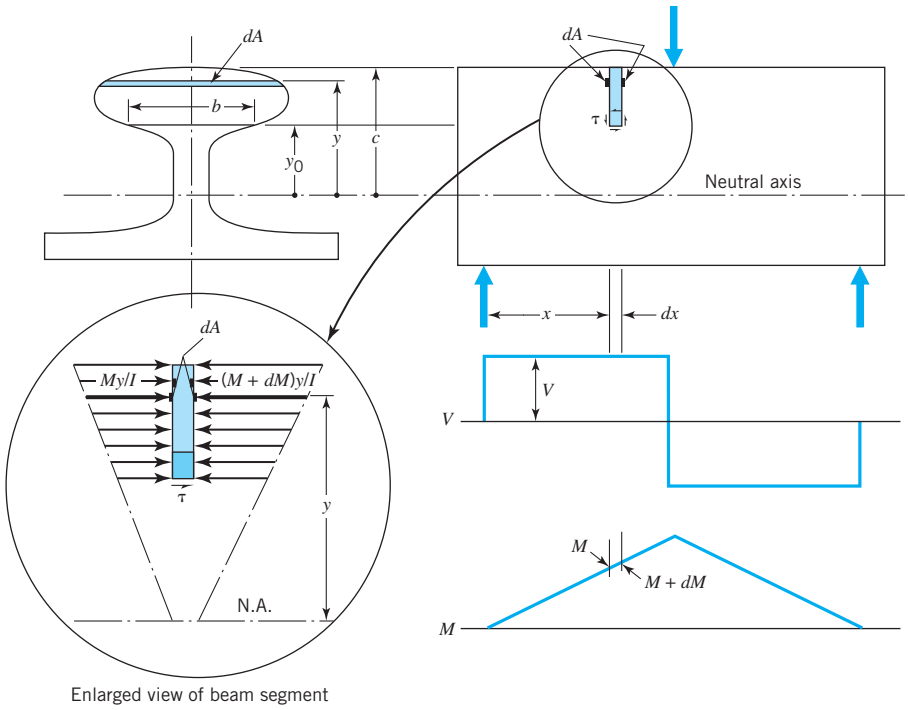

FIGURE 4.14
Analysis of transverse shear stress distribution.

on the right is downward. If only these two vectors acted on the element, it would tend to rotate clockwise. This is prevented by the counterclockwise shear stresses shown on the top and bottom surfaces of the element. The reality of these horizontal shear stresses is easy to visualize: If one loads a book or paper tablet with the forces in Figure 4.14, the pages slide on each other; if the plastic playing cards in a long-unused deck are stuck together, flexing the deck with this three-point beam loading breaks them loose. Coming back to the small element in the figure, we can determine the magnitude of all four shear stresses by evaluating any one of them. We now proceed to evaluate the shear stress on the *bottom* of the element.

Imagine two transverse saw cuts, distance dx apart, starting at the top of the beam and continuing down just to include the sides of the square element. This serves to isolate a segment of the beam, the bottom surface of which is the bottom surface of the element acted upon by shear stress τ. Note that the beam segment involves the full width of the beam. Its bottom surface, acted upon by the unknown shear stress, has a rectangular area of dimensions dx and b. Dimension b will, of course, be different for various values of y_0 (i.e., for various depths of "saw cut").

The enlarged view in Figure 4.14 shows the forces acting on the beam segment. A key point is that the bending stresses are *slightly greater on the right side* where the bending moment is greater than on the left side by amount dM. The unknown shear stress at the bottom must be sufficiently large to compensate for this inequality. Because the sum of horizontal forces must be zero,

$$\int_{y=y_0}^{y=c} \frac{dM\, y}{I}\, dA = \tau b\, dx$$

But $dM = V\,dx$; hence,

$$\int_{y=y_0}^{y=c} \frac{V\,dx\,y}{I}\,dA = \tau b\,dx$$

Solving for τ gives

$$\tau = \frac{V}{Ib}\int_{y=y_0}^{y=c} y\,dA \qquad \textbf{(4.12)}$$

Let us now make a few important observations concerning this equation. First, the shear stress is zero at the top (and bottom) surfaces. This is true because the saw cuts have no depth, so there is no inequality of bending forces on the two sides to be compensated for by shear stress at the bottom. (Looking at it another way, if the small element in the upper right of Figure 4.14 is moved to the very top, then the top surface of the element is part of the free surface of the beam. There is nothing in contact with this surface that could impose a shear stress. If there is no shear stress on the top of the element, the requirements of equilibrium prohibit shear stresses on any of the other three sides.) As the saw cuts acquire increasing depth, larger and larger surfaces are exposed to the inequality of bending stress; hence, the compensating shear stress must increase correspondingly. Note that at the saw cut depth shown in Figure 4.14, a great increase in shear stress would result from cutting just a little deeper (i.e., slightly reducing y_0) because the area over which the compensating shear stress acts is rapidly decreasing (i.e., b decreases rapidly as y_0 is decreased). Note further that the maximum shear stress is experienced at the neutral axis. This is a most gratifying situation! The maximum shear stress exists precisely where it can best be tolerated—at the neutral axis where the bending stress is zero. At the critical extreme fibers where the bending stress is maximum, the shear stress is zero. (A study of Eq. 4.12 indicates that for unusual sections having a width, b, *at* the neutral axis substantially greater than the width *near* the neutral axis, the maximum shear stress will not be at the neutral axis. However, this is seldom of significance.)

It often helps to establish concepts clearly in mind if we can visualize them on a physical model. Figure 4.15 shows an ordinary rubber eraser ruled with a row of elements that indicates relative shear strains (hence, stresses) when the eraser is loaded as a beam (as shown in Figure 4.15*b*). If the eraser is loaded carefully, we can see that the top and bottom elements are negligibly distorted (i.e., the initial right angles remain right angles) while the greatest distortion in the right-angle corners occurs in the center elements.

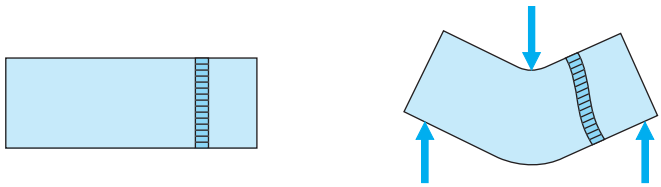

(*a*) Marked and unloaded

(*b*) Loaded as a beam

FIGURE 4.15
Transverse shear strain (hence stress) distribution shown by rubber eraser.

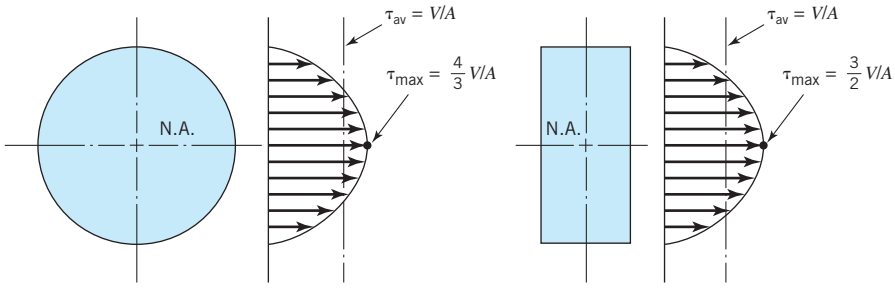

FIGURE 4.16
Transverse shear stress distribution in solid round and rectangular sections.

Applying Eq. 4.12 to solid round and rectangular sections, we find the parabolic shear stress distributions shown in Figure 4.16, with maximum values at the neutral axis for *solid round* sections of

$$\tau_{max} = \tfrac{4}{3} V/A \qquad \textbf{(4.13)}$$

for *solid rectangular* sections of

$$\tau_{max} = \tfrac{3}{2} V/A \qquad \textbf{(4.14)}$$

For a hollow round section, the stress distribution depends on the ratio of inside to outside diameter, but for *thin-wall tubing*, a good approximation of the maximum shear stress is

$$\tau_{max} = 2V/A \qquad \textbf{(4.15)}$$

For a conventional I-beam section, width b is so much less in the web than in the flanges that the shear stresses are much higher in the web. In fact, the shear stresses throughout the web are often approximated by dividing the shear force, V, by the area of the web only, with the web considered as extending the entire depth of the beam.

In the foregoing analysis the tacit assumption was made that the shear stress is uniform across the beam width, b, at any distance, y_0, from the neutral axis (see Figure 4.14). Although not strictly correct, this assumption seldom leads to errors of engineering significance. The variation of shear stress across the width of a beam is treated in [8] and [11]. Another topic left to advanced texts in strength of materials is the loading of beams whose cross sections have no axes.

A final point to be noted is that only in very *short* beams are the transverse shear stresses likely to be of importance *in comparison with the bending stresses*. The principle behind this generalization is illustrated in Figure 4.17, where the same loads are shown applied to a long and short beam. Both beams have the same shear

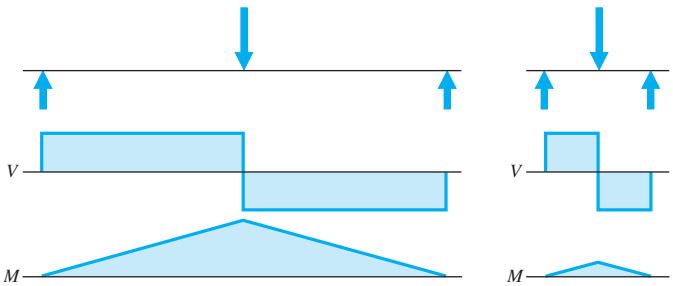

FIGURE 4.17
Effect of beam length on bending and shear loading.

load and the same *slope* of the bending moment diagram. As the beam length approaches zero, the bending moment (and bending stresses) approaches zero, while the shear load and stresses remain unchanged.

SAMPLE PROBLEM 4.2 Determine Shear Stress Distribution

Determine the shear stress distribution for the beam and loading shown in Figure 4.18. Compare this with the maximum bending stress.

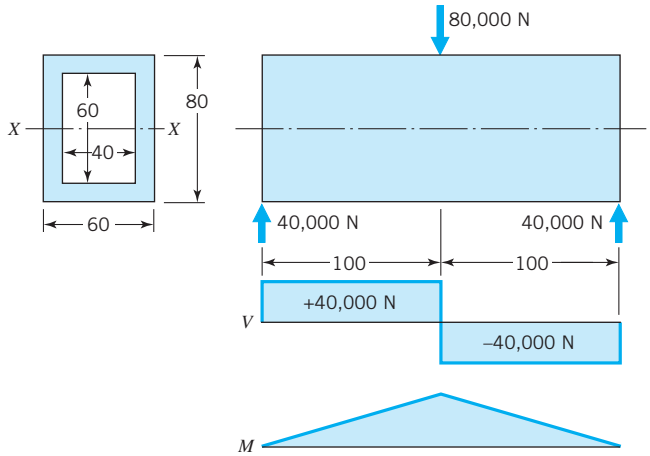

FIGURE 4.18
Sample Problem 4.2. Beam shear stress distribution. Note: all dimensions are in millimeters; section properties are $A = 2400\ \text{mm}^2$; $I_x = 1840 \times 10^6\ \text{mm}^4$.

SOLUTION

Known: A rectangular beam with given cross-sectional geometry has a specified central load.

Find: Determine the shear stress distribution and the maximum bending stress.

Assumptions:

1. The beam is initially straight.
2. The beam is loaded in a plane of symmetry.
3. The shear stress in the beam is uniform across the beam width at each location from the neutral axis.

Schematic and Given Data:

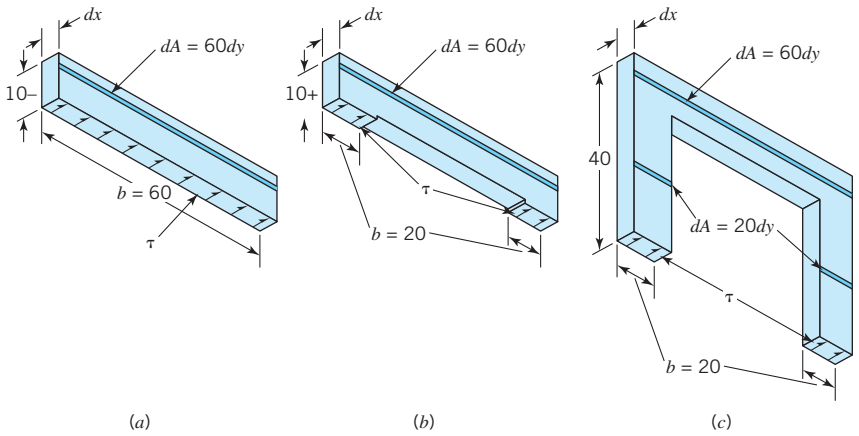

FIGURE 4.19
Sample Problem 4.2 partial solution—τ at three levels.

Analysis:

1. With reference to Figure 4.14 and Eq. 4.12, it is known at the outset that $\tau = 0$ at the top and bottom surfaces. This gives a start in plotting the shear stress distribution in Figure 4.20. As the imaginary parallel saw cuts (described in connection with Figure 4.14) proceed down from the top to increasing depth, the areas exposed to the slightly unbalanced bending stresses increase, thereby causing the compensating shear stress at the bottom of the imaginary segment to increase parabolically. This continues to a saw cut depth of 10 mm. Figure 4.19*a* illustrates the imaginary segment just before the saw cuts break through the interior surface of the section. The shear stress at this level (which acts on bottom area $60 \cdot dx$) is calculated using Eq. 4.12 as

$$\tau = \frac{V}{Ib}\int_{y=y_0}^{y=c} y\,dA = \frac{40{,}000}{(1.840 \times 10^6)(60)}\int_{y=30}^{y=40} y(60dy)$$

$$= \frac{40{,}000}{(1.840 \times 10^6)(60)}(60)\left[\frac{y^2}{2}\right]_{y=30}^{y=40} = 7.61 \text{ N/mm}^2, \text{ or } 7.61 \text{ MPa}$$

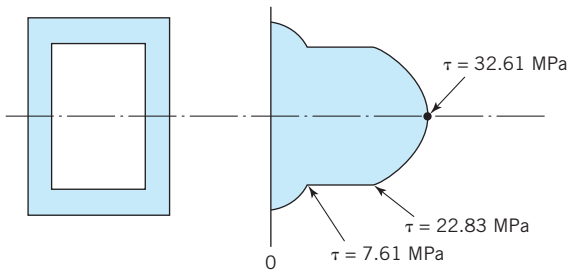

FIGURE 4.20
Plot of shear stress distribution—Sample Problem 4.2.

2. With a slightly deeper saw cut, the inner surface is broken through, and the area over which the shear stress acts is suddenly reduced to 20 *dy*, as shown in Figure 4.19*b*. The unbalanced bending forces acting on the segment sides are virtually unchanged. Thus, the only term that changes in Eq. 4.12 is *b*, which is reduced by a factor of 3, thereby giving a shear stress three times as high, or 22.83 MPa.

3. As the saw cut depth increases until it reaches the neutral axis, the area over which the shear stress acts remains the same, while greater and greater imbalances build up as additional areas *dA* are exposed. But, as shown in Figure 4.19*c*, these added areas *dA* are only one-third as large as those in the top portion of the section. Hence, the increased shear stress at the neutral axis is not as great as might at first be expected. When using Eq. 4.12 to find τ at the neutral axis, note that two integrals are involved, one covering the range of *y* from 0 to 30 mm and the other from 30 to 40 mm. (The latter integral, of course, has already been evaluated.)

$$\tau = \frac{V}{Ib}\int_{y=y_0}^{y=c} y\,dA = \frac{40{,}000}{(1.840\times 10^6)(20)}\left[\int_{y=0}^{y=30} y(20\,dy) + \int_{y=30}^{y=40} y(60\,dy)\right]$$

$$= \frac{40{,}000}{(1.840\times 10^6)(20)}(20)\left[\frac{y^2}{2}\right]_{y=0}^{y=30} + 22.83$$

$$= 32.61 \text{ N/mm}^2, \text{ or } 32.61 \text{ MPa}$$

These calculations enable the shear stress plot in Figure 4.20 to be drawn.

4. By way of comparison, the maximum bending stresses occur in the top and bottom surfaces of the beam, halfway along its length, where the bending moment is highest. Here, the bending stress is computed as

$$\sigma = \frac{Mc}{I} = \frac{(40{,}000\times 100)(40)}{1.84\times 10^6} = 86.96 \text{ N/mm}^2$$

$$= 86.96 \text{ MPa}$$

Comment: Recalling that the shear stress must be zero at the exposed inner surface of the section, it is apparent that the evenly distributed shear stress assumed in Figure 4.19*a* is incorrect, and that the shear stresses in the outer supported portions of the section at this level will be higher than the calculated value of 7.61 MPa. This is of little importance because, to the degree that shear stresses are of concern, attention will be focused at the level just below, where the calculated value of τ is three times as high, or at the neutral axis where it is a maximum.